Synthesis and Characterization of Elastin-Mimetic Protein Gels Derived from a Well-Defined Polypeptide Precursor

R. Andrew McMillan and Vincent P. Conticello*

Department of Chemistry, Emory University, Atlanta, Georgia 30322

Received December 15, 1999; Revised Manuscript Received April 24, 2000

ABSTRACT: To elucidate the effects of uniformity of molecular architecture on gel properties, a protein polymer based on the elastin-mimetic repeat sequence [(Val-Pro-Gly-Val-Gly)$_4$(Val-Pro-Gly-Lys-Gly)], **1** (**Lys-25**), was synthesized using genetic engineering and microbial protein expression. The regularly placed lysine residues in poly(**Lys-25**) underwent selective reaction with electrophilic cross-linkers under mild conditions in either dimethyl sulfoxide or aqueous phosphate buffer to afford solvent-swollen networks. Chemical derivatization and spectroscopic investigations of the cross-linking reaction indicated that approximately 85% of the lysine residues reacted with the cross-linker. The protein hydrogel exhibited reversible, temperature-dependent expansion and contraction with an estimated midpoint temperature for the phase transition at 35 °C. Scanning electron microscopy (SEM) investigations indicated profound differences in morphology between protein gels prepared in organic vs aqueous solution.

Introduction

Hydrogels are cross-linked, water-swollen polymer networks that have great technological importance as biomedical materials. Biocompatible polymer hydrogels are employed in medical applications as prosthetic devices, soft contact lenses, drug delivery agents, and matrices for cell encapsulation and tissue engineering.[1] Control of network architecture is an important consideration in the design of polymer materials for many of these applications as it dramatically affects biomedically important gel properties including solute permeability, equilibrium swelling ratio, and viscoelasticity.[2] However, most polymer networks have a statistical distribution of cross-link sites due to random incorporation of multifunctional or cross-linkable monomers into the polymer during synthesis. Consequently, synthetic hydrogels have irregular architectures with a distribution of microenvironments and pore sizes within the network.[3] This nonuniform topology certainly has an influence on macromolecular properties and performance of these materials; although, the importance of this effect has not been explored experimentally due to the inability to specify the position of the cross-link sites.

Naturally occurring polypeptides also form cross-linked networks that are formally analogous to synthetic polymer hydrogels and elastomers.[4,5] Biopolymer networks are utilized in natural systems as the flexible components of soft tissues and protein fibers. In contrast to synthetic or semisynthetic polymer networks, these natural biopolymer networks are derived from proteins that have well-defined sequences, usually comprising tandem repeats of oligopeptide motifs with limited plasticity in the repeat sequence. The repetitive sequence pattern can induce a regular secondary structure into the polypeptide that may directly influence the macromolecular properties of the network (vide infra). These polypeptides are posttranslationally cross-linked into a network, usually via enzymatic modification of the side chains of specific amino acids. The sequence of the polypeptide determines the positions of the cross-links, which usually occur at well-defined intervals along the polypeptide chain. The structural uniformity of these natural elastic materials is presumably responsible for their unique materials properties, i.e., the high resilience and nearly ideal elastic behavior of several protein rubbers.[4] Indeed, the biological function of these materials may depend integrally on this structural specificity. For example, high resilience in an elastomeric material prevents dissipation of energy as heat, which could cause catastrophic failure of the biomaterial under normal usage conditions. The evolutionary conservation of repeat sequence in natural bioelastomeric materials implies a strong correlation between macromolecular architecture and the materials properties essential for correct performance of biological function.

Natural bioelastomers can serve as paradigms for the design of synthetic protein-based hydrogels that retain the sequence definition and structural uniformity of the former materials, but permit introduction of functional groups that facilitate in vitro formation of extended networks *under controllable conditions*. Our strategy for the preparation of well-defined, synthetic polypeptide networks involves two steps: (1) the genetically directed synthesis of repetitive precursor polypeptides of uniform and controllable macromolecular architecture and (2) the chemical cross-linking of these macromolecules into networks through selective reaction of specific amino acid side chains. Using this biomimetic approach, the architectural parameters that have a critical impact on network properties, i.e., polypeptide chain length, consensus repeat sequence, and cross-link position and density, may be specified in these synthetic networks to a similar extent as observed for bioelastomers. The effect of sequence uniformity on the structure and macromolecular properties of polymer networks can be examined using this strategy, which may ultimately permit tailoring of the materials properties of the network through manipulation of the polypeptide sequence at the genetic level.

Protein polymers of defined sequence have been prepared by recombinant DNA (rDNA) technology and bacterial protein expression with near-absolute control of macromolecular architecture, i.e., size, composition,

* To whom correspondence should be addressed at vcontic@emory.edu.

10.1021/ma9921091 CCC: $19.00
Published on Web 06/07/2000

sequence, topology, and stereochemistry.[6] These biosynthetic poly(α-amino acids) may be considered as model uniform polymers and can possess unique structures, and hence materials properties, as a consequence of their sequence specificity. In addition, the uniform architecture of these biosynthetic protein polymers facilitates the analysis of structure−property relationships and, ultimately, the control of materials properties. Protein polymers have been designed that selectively self-assemble into dimensionally defined lamellar crystallites,[7] lyotropic smectic mesophases,[8] and thermoreversible gels[9] on the basis on structural features programmed into the polypeptide sequence at the molecular level. In contrast, most synthetic polymers comprise heterogeneous populations of chains and consequently display a range of structures and physical properties under comparable conditions in solution and in the solid state.[10]

We previously described the construction and expression of concatameric genes that encode polymers of repeat sequence [(Val-Pro-Gly-Val-Gly)$_4$(Val-Pro-Gly-Lys-Gly)], **1** (**Lys-25**), and the isolation and preliminary characterization of the corresponding protein polymer, poly(**Lys-25**).[11] We report herein the large-scale synthesis and detailed characterization of poly(**Lys-25**) and the preparation and characterization of responsive hydrogels from poly(**Lys-25**) by cross-linking under environmentally benign conditions. The protein polymer poly(**Lys-25**) provides a uniform context for evaluation of the effects of cross-linking reaction parameters (temperature, concentration, ionic strength, and cross-linker identity) on the degree of cross-link formation, morphology, and macroscopic responsive behavior of biomimetic hydrogels.

Experimental Methods

Materials and Methods. The preparation of the recombinant *Escherichia coli* expression strains BLR(DE3)(pRAM**1**) and BLR(DE3)(pRAM**2**) has been previously described.[11] Bis(sulfosuccinimidyl) suberate, disuccinimidyl suberate, and sulfosuccinimidyl-4-*O*-(4,4′-dimethoxytrityl) butyrate (sulfo-SDTB) were purchased from Pierce Chemical Co. (Rockford, IL). Isopropyl-*β*-D-thiogalactopyranoside (IPTG) was purchased from Calbiochem, Inc. (San Diego, CA). Tetracycline, carbenicillin, benzonase, lysozyme, and phenylmethylsulfonyl fluoride (PMSF) were obtained from the Sigma Chemical Co. (St Louis, MO). L-Lysine bis(hydrochloride) (ϵ-^{15}N, 98+%) was obtained from Cambridge Isotope Laboratories, Inc. (Andover, MA). The procedures for manipulation of DNA, transformation of competent cells, and growth and induction of bacterial cultures were adapted from published literature[12] or from instructions supplied by manufacturers. All reagents for the manipulation of bacteria and proteins were sterilized either by autoclave or passage through a 0.22 μm PES filter. Protein electrophoresis was performed using 10−15% gradient discontinuous SDS polyacrylamide gels on a PhastSystem apparatus from Amersham Pharmacia Biotech, Inc. (Piscataway, NJ) and was visualized with the silver staining process supplied by the manufacturer.

Physical and Analytical Measurements. Solution NMR spectra were recorded on either a GE Omega 600 (600 MHz, ^{1}H) or a Varian INOVA 400 (400 MHz, ^{1}H; 100.6 MHz, ^{13}C; 40.5 MHz, ^{15}N) instrument. Chemical shifts for ^{1}H and ^{13}C NMR spectra were referenced and reported relative to internal sodium 2,2-dimethyl-2-silapentane-5-sulfonate (DSS). Chemical shifts for ^{15}N NMR spectra in solution were referenced to an external standard of 1 M urea (^{15}N, 98+%) in dimethyl sulfoxide (77.0 ppm) and reported relative to liquid ammonia (0 ppm).[13] Standard suppression techniques were employed to reduce the signal due to the residual protons of water in the ^{1}H NMR of aqueous solutions. Solid-state CP/MAS ^{13}C and VACP/MAS ^{15}N NMR spectra were recorded on a Bruker DSX 400 spectrometer (100.6 MHz, ^{13}C; 40.5,^{15}N) at the Georgia Institute of Technology. Solid-state ^{13}C chemical shifts were referenced to the methylene carbons of external adamantane (31.26 ppm) and reported relative to the methyl resonances of an external sample of aqueous DSS (0 ppm). Variable amplitude (VA)CP/MAS ^{15}N NMR spectra were collected at a spinning speed of 4500 Hz and a contact time of 5 ms. Solid-state ^{15}N NMR shifts were referenced to an external standard of 10% urea (^{15}N, 98+%) in dimethyl sulfoxide (79.4 ppm) and reported relative to external liquid ammonia (0 ppm).[13] The NMR data were processed using the program FELIX from Molecular Simulations, Inc. (San Diego, CA) on a Silicon Graphics Octane workstation.

Quantitative analyses of the solid-state ^{15}N NMR spectra of the lyophilized hydrogel were performed using the standard model for evolution of induced magnetization (M) on contact time (τ) in the CP/MAS experiment.[14] Spectra were recorded at 15 contact times between 0 and 5 ms, and the magnetizations of the reacted (amide) and unreacted (amine) ^{15}N nuclei were plotted as a function of contact time using the graphics program SigmaPlot 5.0 from SPSS, Inc. (Chicago, IL). The resulting data for both unreacted and reacted nitrogen nuclei were fit to eq 1 where M_0 is the nitrogen magnetization in the

$$M(\tau) = [M_0/(1 - \lambda)][\exp(-\tau/T_{1\rho H}) - \exp(-\tau/T_{CP})] \quad (1)$$

absence of spin−lattice relaxation, $T_{1\rho H}$ is the spin−lattice relaxation time of protons in the rotating frame, T_{CP} is the cross-polarization time constant, and λ is the ratio $T_{CP}/T_{1\rho H}$. The fractional composition of reacted and unreacted ^{15}N nuclei in the hydrogel were calculated from the ratios $[M_0^R/(M_0^R + M_0^U)]$ and $[M_0^U/(M_0^R + M_0^U)]$, respectively.

Temperature-dependent turbidimetry measurements were performed in an Ultrospec 3000 UV/visible spectrophotometer equipped with a programmable Peltier cell and temperature control unit from Amersham Pharmacia Biotech, Inc. (Piscataway, NJ). The inverse temperature transition of elastin-mimetic polypeptides (concentrated 0.5−1.0 mg/mL) was monitored at 256 nm at a ramp rate of 1 °C/min in both forward and reverse directions. Spectra were analyzed by SWIFT−T_m applications software from Amersham Pharmacia Biotech, Inc. Fourier-transform infrared (FTIR) spectra were recorded on a MAGNA-IR 560 E.S.P. spectrometer from Nicolet Instrument Corp. (Madison, WI). Absorption maxima were assigned using the second derivative and Fourier self-deconvolution analyses in the OMNIC E.S.P. software package supplied by the manufacturer.

Digital video image capture was used to monitor the transitions of hydrogel specimens. A square sample of a cast hydrogel (aspect ratio > 10) was immersed in a cell containing distilled, deionized water, which was maintained at constant temperature by a refrigerated circulating bath. The temperature of the cell was determined directly from an immersed copper−constantan thermocouple. Gel opacity measurements were determined as a function of temperature from a uniform area of the specimen. Static images of the hydrogels were acquired on a matte black (carbon tape) background with a Panasonic CL324 digital camera interfaced to a Silicon Graphics O2 video workstation. Image analyses were performed on a Macintosh computer using the public domain NIH Image program (developed at the U.S. National Institutes of Health and available on the Internet at http://rsb.info.nih.gov/nih-image/). Each grayscale TIFF image was inverted such that the black background would have a pixel value of zero (white). The average pixel value was determined from three consecutive measurements of the selected area. The average gel opacity values were measured on a scale from 0 to 255 (white to black), in which the larger pixel value corresponded to a greater optical density in the specimen. The fidelity of the optical density determinations for each measurement was checked with a Kodak T-14 control swatch that was placed next to the sample cell in each digital image. Analysis of the

control swatch at different temperatures afforded a value of 5.76 for the mean standard deviation in the optical density determinations.

High-resolution scanning electron microscopy (HRSEM) was employed to characterize the morphology of gel specimens. The specimens were prepared for imaging by the critical point drying technique. Solvent-swollen specimens of the cross-linked networks were desolvated with increasing concentrations of ethanol in the swelling solvent (either dimethyl sulfoxide or water). The water-swollen gel was cycled between 4 and 40 °C during each exchange step to ensure adequate perfusion of the gradient mixtures into the specimen. The ethanol in the gels was exchanged with liquid carbon dioxide in a Polaron critical point drying apparatus, and the CO_2 was removed above its critical temperature and pressure. The dried gels were immobilized on double-sided carbon tape and a thin (10−20 nm) film of gold/palladium (60:40) alloy was applied with an Emscope sputter coater (7.5 mA, 50 mTorr, 3 min). Specimens were topographically imaged in the below-lens configuration with an ISI DS-130 scanning electron microscope equipped with a LaB_6 electron source.

Amino acid compositional analyses were obtained from the Microchemical Facility of the Winship Cancer Center at Emory University. MALDI−TOF mass spectra of poly(**Lys-25**) and poly(**Ile-25**) were recorded on a PerSeptive Biosystems Voyager spectrometer at the Protein/DNA Technology Center of Rockefeller University.

Large Scale Expression of Protein Polymers. Single colonies of *E. coli* expression strain BLR(DE3)(pRAM**1**) were used to inoculate eight seed cultures of LB medium (50 mL) containing carbenicillin (50 μg/mL) and tetracycline (30 μg/mL). These cultures were grown to saturation at 37 °C and centrifuged at 4000*g* and 4 °C for 20 min, and the individual cell pellets were resuspended in 100 mL of sterile LB medium. The resuspended seed cultures were used to inoculate 8 × 1 L of sterile LB medium supplemented with carbenicillin (50 μg/mL) and tetracycline (30 μg/mL) in 2.8 L Fernbach flasks. The cultures were incubated at 37 °C with agitation at 200 rpm until the $OD_{600} \approx 1$. An aliquot of aqueous 0.1 M IPTG was added to each culture to induce target protein synthesis at a final concentration of 1 mM IPTG. After a 3 h induction period (final $OD_{600} \approx 1.7$ AU), the cultures were combined and the cells were isolated by centrifugation at 4000*g* at 4 °C for 20 min. The collected cells were lysed by three successive freeze/thaw cycles (−80/+25 °C), and were resuspended in 400 mL of lysis buffer (50 mM Tris−HCl, 100 mM NaCl, 1 mM EDTA pH 7). Lysozyme was added to a final concentration of 1 mg/mL, and the suspension was incubated on ice for 30 min. The solution was sonicated in 3 s pulses at 20 kHz for 1 min, and 1 μL of benzonase (300 U/μL) was added to the lysate. The mixture was warmed to ambient temperature and 100 mM phenylmethylsulfonyl fluoride was added to a final concentration of 1 mM. The whole cell lysate was centrifuged at 20000*g* for 20 min at 4 °C, and the soluble supernatant was separated from the insoluble cell debris. The protein polymer was precipitated from the supernatant by addition of an equivalent amount of 2× precipitation buffer (100 mM CAPS, 1 M NaCl, pH 10) and equilibrated at 40 °C for 30 min. The precipitate was isolated by centrifugation of the mixture at 15000*g* at 40 °C for 15 min. The protein was resuspended in a minimal amount of distilled, deionized water at 4 °C and furthur purified by repeated precipitation with 1× precipitation buffer until only one band was observed by discontinuous 10−15% gradient SDS−PAGE. Lipids and other endotoxins were removed by extraction of the final aqueous protein solution with 2 × 400 mL of carbon tetrachloride. The purified protein was concentrated and desalted by centrifugal ultrafiltration (Pall Filtron Corp., MWCO ≈ 30 kDa). Lyophilization of the retentate afforded the protein as a colorless, spongy mass. The isolated yield of the poly(**Lys-25**) fusion polypeptide was 64 mg/L culture.

The isotopically enriched protein polymer poly(**^{15}N-Lys-25**) was prepared via a modification of the procedure for poly(**Lys-25**). Ten seed cultures of *E. coli* strain BLRDE3(pRAM**1**) in sterile LB medium (100 mL) were used to inoculate 1 L each of M9 medium supplemented with carbenicillin (50 μg/mL) and tetracycline (30 μg/mL) and all proteinogenic amino acids except lysine (20 μg/mL each). The cultures were incubated at 37 °C with moderate agitation (200 rpm) until the OD_{600} reached approximately 0.5 AU. An aqueous solution (1 mL) of ϵ-^{15}N-L-lysine bis(hydrochloride) (50 mg/mL) was added to each liter of culture. The cultures were incubated for an additional 30 min at 37 °C, and an aliquot of aqueous 0.1 M IPTG was added to each culture to a final concentration of 1 mM IPTG. The cultures were incubated at 37 °C for an additional 3 h. The cells were harvested by centrifugation at 4 °C and 4000*g* for 20 min. The labeled protein was isolated as a colorless, spongy solid from the cell lysate as described above. The yield of purified poly(**^{15}N-Lys-25**) fusion protein was 23 mg/L of culture.

The poly(**Ile-25**) fusion protein was prepared from expression of a 6 L culture of *E. coli* strain BLR(DE3)(pRAM**2**) as described above for poly(**Lys-25**). The protein was purified from the whole cell lysate in a similar procedure by three temperature-dependent precipitation cycles from TN buffer (50 mM Tris−HCl pH 7.5, 500 mM NaCl). The yield of poly(**Ile-25**) fusion polypeptide from this procedure was 98 mg/L of culture.

Cyanogen Bromide Cleavage. The same general protocol was employed for removal of the decahistidine tags from either poly(**Lys-25**), poly(**^{15}N-Lys-25**), or poly(**Ile-25**). The fusion polypeptide (200−500 mg) was dissolved in 90% formic acid and water was added to adjust the concentration to 70% formic acid (final concentration of protein = 1 mg/mL). Cyanogen bromide was added to the mixture at a final concentration of 5 mg/mL. The reaction mixture was sparged with argon for 15 min to displace dissolved oxygen. The reaction vessels were sealed under argon, covered with aluminum foil, and stirred for 24 h at ambient temperature. Distilled, deionized water (250 mL) was added to the mixture, and the volatiles were removed by rotary evaporation under dynamic vacuum (ca. 1 mmHg). This procedure was repeated three times to ensure complete removal of formic acid from the protein polymer. The cleavage products were resuspended in a minimal amount of distilled, deionized water and the decahistidine tag was removed by centrifugal ultrafiltration using Centricon concentrators (MWCO ≈ 30 kD). The protein polymers were isolated as colorless spongy solids after lyophilization. Yield: poly(**Lys-25**), 86%; poly(**^{15}N-Lys-25**), 87%; poly(**Ile-25**), 84%. Poly(**Lys-25**). Amino acid analysis. Calcd: Gly, 40%; Lys, 4%; Pro, 20%; Val, 36%. Found: Gly, 39.9%; Lys, 4.1%; Pro, 19.5%; Val, 36.5%. FTIR (KBr): 1693, 1661, 1628 (amide I); 1553, 1532 (amide II); 1283, 1264 (amide III) cm^{-1}. Poly(**^{15}N-Lys-25**). Amino acid analysis. Calcd: Gly, 40%; Lys, 4%; Pro, 20%; Val, 36%. Found: Gly, 39.2%; Lys, 4.2%; Pro, 19.6%; Val, 36.6%. ^{15}N NMR (70% H_2O/30% D_2O): 32.1 ppm. Poly(**Ile-25**). Amino acid analysis. Calcd: Gly, 40%; Ile, 4%; Pro, 20%; Val, 36%. Found: Gly, 39.1%; Ile, 4.2%; Pro, 19.5%; Val, 36.8%. FTIR (KBr): 1690, 1661, 1625 (amide I); 1550, 1534 (amide II); 1282, 1260 (amide III) cm^{-1}. ^{1}H and ^{13}C NMR chemical shift assignments for poly(**Lys-25**) and poly(**Ile-25**) are summarized in Tables 1 and 2, respectively.

Chemical Cross-linking of Protein Polymers. Purified, cleaved poly(**Lys-25**) (25 mg, 12 mequiv) was dissolved in 400 μL of cross-linking buffer (20 mM phosphate, pH 8.5). The mixture was shaken at 4 °C on a vortex mixer until dissolved and was incubated on ice until use. Meanwhile, bis(sulfosuccinimidyl) suberate (3.4 mg, 6.0 mmol) was dissolved in 100 μL of cross-linking buffer and incubated on ice. The solutions were added together at 4 °C, mixed by vortex, and briefly centrifuged to remove entrapped air bubbles. The reaction mixture was warmed to ambient temperature (approximately 25 °C) to facilitate the cross-linking reaction. After approximately 10 min, an opaque gel had formed in the reaction vessel. The mixture was incubated for 24 h at ambient temperature. The reaction byproducts were removed from the gel by successive washes with distilled, deionized water (1.5 mL) at 0 and 45 °C, respectively. The gels were stored at 4 °C as swollen specimens in distilled, deionized water (1.5 mL). An identical procedure was used to prepare a cross-linked gel

Table 1. ^{1}H NMR Chemical Shift Assignments for Poly(Lys-25) and Poly(Ile-25) (ppm vs Internal DSS)

residue	NH	α-H	β-H	other
		Poly(**Lys-25**)		
Val[1]	8.05	4.44	2.09	γ_{CH_2} 0.92, 0.97
Pro[2]		4.40	1.95, 2.30	γ_{CH_2} 1.99
				δ_{CH_2} 3.70, 3.90
Gly[3]	8.47	3.96		
Val[4]	8.00	4.16	2.09	γ_{CH_3} 0.93, 0.94
Lys[4]	8.23	4.37	1.87, 1.77	γ_{CH_2} 1.34, 1.45
				δ_{CH_2} 1.68
				ϵ_{CH_2} 2.98
				$\epsilon_{NH_3^+}$ 7.55
Gly[5]	8.53	3.92	–	
		Poly(**Ile-25**)		
Val[1]	8.04	4.43	2.07	γ_{CH_3} 0.92, 0.97
Pro[2]		4.40	1.92, 2.29	γ_{CH_2} 1.98
				δ_{CH_2} 3.70, 3.90
Gly[3]	8.47	3.95		
Val[4]	7.98	4.15	2.07	γ_{CH_3} 0.93, 0.95
Ile[4]	8.00	4.23	1.77, 1.89	γ_{CH_2} 1.19, 1.45
				γ_{CH_3} 0.91
				δ_{CH_3} 0.86
Gly[5]	8.52	3.93		

Table 2. ^{13}C NMR Chemical Shift Assignments for Poly(Lys-25) and Poly(Ile-25) (ppm vs internal DSS)

residue	CO	α-C	β-C	other
		Poly(**Lys-25**)		
Val[1]	174.6	59.8	32.6	γ_C 20.2, 20.9
Pro[2]	177.4	63.4	32.1	γ_C 27.4
				δ_C 51.0
Gly[3]	173.5	44.9		
Val[4]	176.6	62.3	32.6	γ_C 20.4, 20.9
Lys[4]	176.9	56.2	33.1	γ_C 24.8
				δ_C 30.9
				ϵ_C 42.4
Gly[5]	174.0	45.0		
		Poly(**Ile-25**)		
Val[1]	174.4	59.6	32.6	γ_C 20.2, 20.9
Pro[2]	177.2	63.3	31.2	γ_C 27.3
				δ_C 50.8
Gly[3]	173.4	44.9		
Val[4]	176.4	62.1	32.6	γ_C 20.4, 20.9
Ile[4]	176.5	60.9	38.6	γ_{CH_2} 27.0
				γ_{CH_3} 17.4
				δ_{CH_3} 12.8
Gly[5]	173.8	45.0		

from poly(**^{15}N-Lys-25**). Specimens for CP/MAS NMR studies were dried by lyophilization, which afforded colorless spongy solids. For optical density measurements, the reaction mixture was cast at 10 °C into a mold consisting of two glass plates and a Teflon spacer (0.7 mm thick) lightly coated with Cello-Seal grease. The surfaces of the glass plates were pretreated with a 10% (w/v) solution of dimethyldichlorosilane in dichloromethane to prevent adhesion of the gel. The reaction mixture was incubated in the mold at 25 °C for 24 h, and the resulting gel was rinsed with distilled water and stored as described above. FTIR (KBr): 1693, 1658, 1629, 1615 (amide I); 1549, 1532 (amide II); 1283, 1260 (amide III) cm^{-1}.

Poly(**Lys-25**) was cross-linked in DMSO by dissolving the protein polymer (25 mg, 12 mequiv) in 400 μL anhydrous DMSO and cooling to 16 °C in a microfuge tube. Disuccinimidyl suberate (2.2 mg, 6.0 mmol) was dissolved in 100 μL of anhydrous DMSO and the solution incubated at 16 °C. The two solutions were mixed at 16 °C as above, and the reaction was allowed to proceed at room temperature as before. After approximately 10 min, the reaction mixture had formed an optically transparent gel. These specimens were used directly for microscopy studies and for quantitation of the residual amino groups. Both cross-linking reactions were performed with poly(**Ile-25**) as a non-cross-linkable control polymer. Gelation of the reaction mixture was not observed for poly(**Ile-25**) in either solvent under the conditions described above.

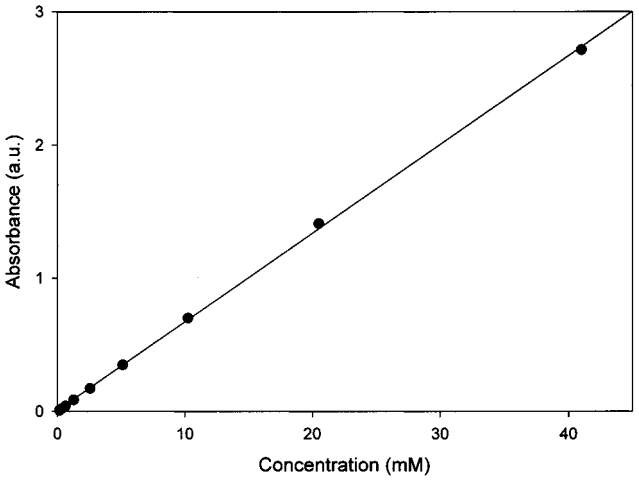

Figure 1. Standard curve of absorbance at 498 nm vs theoretical dimethoxytrityl cation concentration for determination of residual amine content in elastin-mimetic protein gels (error bars are smaller than the symbols for the data points).

Quantitation of Residual Amino Residues. The fraction of residual amino groups within the gels was determined using an adaptation of the method of Cook et al.,[15] for quantitation of surface reactive amino groups on solid polymer specimens. A stock solution of sulfosuccinimidyl-4-*O*-(4,4′-dimethoxytrityl) butyrate (sulfo-SDTB) was prepared by dissolving 5.6 mg (9.2 mmol) of the reagent in 250 μL of dimethylformamide and addition of this solution to 2 mL of 50 mM sodium bicarbonate solution, pH 8.5. An aliquot (200 μL) of this stock solution was added to 2 mL of 35% perchloric acid. Serial dilution of the stock solution (200 μL) into an equal volume of 35% perchloric acid afforded a series of dimethoxytrityl cation standards having concentrations of 84, 42, 21, 10.4, 5.2, 2.6, 1.3, 0.64, 0.32, and 0.16 nmol/mL, respectively. The absorbances of these standard solutions of dimethoxytrityl cation were determined at a wavelength of 498 nm. Three separate measurements were conducted for each concentration, and the average absorbance values were plotted vs theoretical cation concentration using the SigmaPlot program (Figure 1). A least-squares analysis was used to fit a line through the data points (y intercept = 0.069; slope = 15.0; correlation = 1).

The total amine content of a non-cross-linked sample of poly(**Lys-25**) (2.5 mg, 1.2 mequiv) was determined as a benchmark for analysis of the hydrogel specimens. The protein sample was suspended in 400 μL of assay buffer (4.1 mM sulfo-SDTB in 50 mM sodium bicarbonate, pH 8.5) in a 1.5 mL microfuge tube. An excess of sulfo-SDTB, vis-à-vis the theoretically available lysine residues, was initially present in the mixture to ensure complete derivatization of the amine groups of the polymer. The mixture was incubated at ambient temperature for 20 min with moderate agitation. The temperature of the solution was raised to 37 °C to induce coacervation of the polypeptide, and the derivatized protein was collected by centrifugation at 14000g for 10 min at 40 °C. The coacervate was dissolved in 500 μL of distilled, deionized water at 4 °C, washed, and reprecipitated at 40 °C. This process was performed thrice to remove residual sulfo-SDTB from the solution. The reaction mixture was checked for residual sulfo-SDTB by mixing 400 μL aliquots of the supernatant from the wash with equal volumes of 35% perchloric acid, and measuring the absorbance at 498 nm. After the final wash (OD_{498} = 0.003), the product was resuspended in distilled, deionized water (400 μL), and 35% perchloric acid (600 μL) was added to the mixture. The solution turned bright orange due to the hydrolytic release of the dimethoxytrityl cation. The resultant solution was centrifuged at 14000g for 10 min at 4 °C. Serial dilution of the initial aliquot of the supernatant with 35% perchloric acid generated a set of dimethoxytrityl cation concentrations. The absorbances were measured at 498 nm for these solutions, and the corresponding dimethoxytrityl

cation concentrations were determined from the standard plot after adjusting by the appropriate dilution factors. The total amine concentration of the polymer specimen was determined by assuming a one-to-one ratio of amine to dimethoxytrityl cation. The average absorbance of the adjusted dimethoxytrityl cation concentrations was defined on the plot as a 100% amine content, i.e., no substitution of lysine amino groups of poly(**Lys-25**) prior to the analysis.

Poly(**Lys-25**) (2.5 mg) was cross-linked into a gel by addition of an equivalent molar amount of bis(sulfosuccinimidyl) suberate as described above. The washed gel was immersed in 400 μL of assay buffer (4.1 mM sulfo-SDTB in 50 mM sodium bicarbonate, pH 8.5) and repeatedly heated to 45 °C and cooled to 0 °C for 2 h to ensure adequate perfusion of buffer throughout the gel. The liquid was removed, and the derivatized gel was washed successively with 10 aliquots of distilled, deionized water (1.5 mL). Each wash was cycled between 45 and 0 °C to ensure perfusion of the wash water into the gel. Aliquots from each wash (500 μL) were mixed with equal volumes of 35% perchloric acid, and the absorbance at 498 nm was measured. The washing steps were repeated until the orange color of the dimethoxytrityl cation was undetectable ($OD_{498} < 0.005$) to eliminate the error arising from residual, unreacted sulfo-SDTB in the final determination. After removal of residual sulfo-SDTB was complete, the gel was immersed in 35% perchloric acid (600 μL). The temperature was cycled between 0 and 45 °C 10 times to ensure adequate perfusion of the acid into the network. The absorbance of the supernatant was measured at 498 nm for several different dilutions in 35% perchloric acid, and the dimethoxytrityl cation concentration was determined for each dilution. After correction for the appropriate dilution ratios, the results were averaged, and the residual amine content was determined from the standard curve of dimethoxytrityl cation concentrations. The residual amine content was estimated as 12 ± 3.1% of the theoretical value for unsubstituted poly(**Lys-25**), which implies that approximately 88% of the lysine residues originally present in poly(**Lys-25**) reacted with the cross-linker during the formation of the gel. A similar analysis was performed on a gel prepared in DMSO, although the solvent was removed prior to the analysis by exchange with ethanol, lyophilization, and re-swelling in distilled, deionized water (1.5 mL). The residual amine content was determined as above, and was estimated as 17 ± 2.1% of the theoretical value (83% substitution during the cross-linking reaction) for gels formed in DMSO under the previous reaction conditions.

Results and Discussion

Protein Polymer Design. Protein polymers of [(Val-Pro-Gly-Val-Gly)$_4$(Val-Pro-Gly-Xaa-Gly)] (Xaa = Lys, **1**; Ile, **2**) were designed to investigate the effects of structural uniformity, in particular the regular positioning of cross-linkable sites, on the preparation and physical properties of polymer hydrogels.[11] The design of the repeat unit **1** incorporates the two structural criteria necessary for the formation of a polymer hydrogel: (1) a flexible, hydrophilic (polyamide) backbone and (2) chemically reactive, selectively cross-linkable functional groups, i.e., the ϵ-amino substituent of the lysine side chain (Figure 2).[1] Repeat unit **2** was designed as a nonreactive analogue of repeat unit **1** for use as a negative control in the cross-linking studies. The amino acid sequences of **1** and **2** are modeled on the pentapeptide repeat (Val-Pro-Gly-Val-Gly) of bovine and porcine elastin, which has been postulated as the structural basis for the elastomeric behavior of native elastic fiber.[16]

Elastin-mimetic protein polymers [(Val-Pro-Gly-Xaa-Gly)$_n$] display reversible, temperature-dependent phase behavior in aqueous solution.[16] Spontaneous phase separation occurs above a lower critical solution temperature T_t, which results in the formation of polymer-

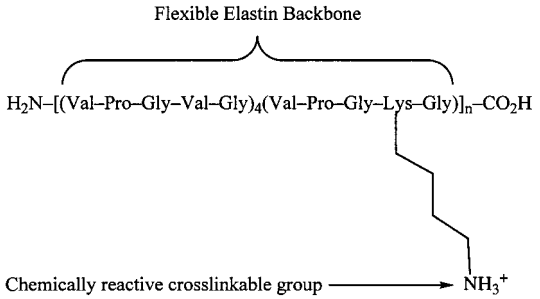

Figure 2. Design of the repeat sequence of the cross-linkable, elastin-mimetic protein polymer poly(**Lys-25**). In the repeat sequence of poly(**Ile-25**), an isoleucine residue replaces the lysine residue of poly(**Lys-25**).

dilute and polymer-rich (coacervate) phases.[17] This process, known as an inverse temperature transition, coincides with a conformational rearrangement of the pentapeptide segments from random coil to type II β-turn.[16] The temperature-dependent phase behavior of elastin-mimetic protein polymers in aqueous solution is formally analogous to that of environmentally responsive polymers such as poly(*N*-isopropylacrylamide),[18] which undergoes entropy-driven dehydration and phase separation above a lower critical solution temperature (LCST). Although the mechanisms of hydrophobic assembly presumably differ between these two materials,[16] their phase behavior can be similarly described using the classical Flory−Huggins theory of polymer solutions.[19] Polymers displaying this type of solution phase behavior have been cross-linked into environmentally responsive hydrogels. These hydrogels undergo discontinuous changes in swollen volume at the phase transition, which may be induced by incremental alterations of environmental conditions such as temperature, pH, and ionic strength.[16] One may envision that the greater uniformity of network architecture, i.e., macromolecular size, cross-link position, and cross-link density available in protein polymers, may lead to greater control over the macroscopic properties, e.g., the sharpness of the volume transition, for responsive gels derived from biosynthetic elastin-mimetic polypeptides.

Large Scale Expression of Protein Polymers. We previously reported the construction of two expression plasmids, pRAM**1** and pRAM**2**, which incorporate concatameric genes of 3000 and 1300 base pairs that encode protein polymers comprising repeats of elastin-mimetic sequences **1** and **2**, respectively.[11] The protein polymers poly(**Lys-25**) and poly(**Ile-25**) were expressed in *E. coli* strain BLR(DE3) after transformation with the recombinant plasmids pRAM**1** or pRAM**2**. Large-scale, batch fermentation (6−8 L of LB medium) afforded yields of 64 and 98 mg of purified polypeptide per liter of culture (4 g of wet cells/L of culture), respectively, as translational fusions to an amino terminal decahistidine tag. The proteins were isolated and purified using the reversible, temperature-dependent precipitation method, which was first developed by Urry et al., for purification of recombinant elastin-mimetic protein polymers from *E. coli* cell lysates.[20] Poly(**^{15}N-Lys-25**), which is isotopically enriched in the reactive lysine side chain, was prepared by an inducible expression of *E. coli* strain BLR(DE3)pRAM**1** in M9 medium supplemented with ϵ-^{15}N-L-lysine (98+%) and purified using the same procedure as for poly(**Lys-25**). Cyanogen bromide cleavage of the fusion proteins afforded poly(**Lys-25**), poly(**^{15}N-Lys-25**), and poly(**Ile-25**) in high yield. Amino acid

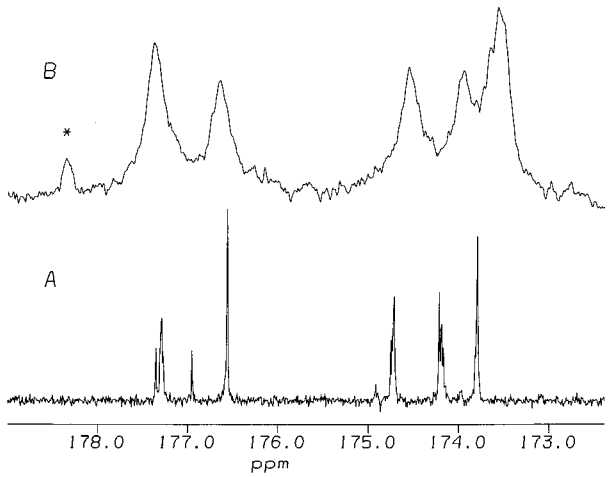

Figure 3. Detail of the amide carbonyl resonances in the ^{13}C NMR spectrum (100 MHz) of poly(**Lys-25**) in 70% H_2O/30% D_2O solution before (A) and after (B) the cross-linking reaction. The position of the nascent carbonyl carbon of the amide cross-link in the hydrogel derived from poly(**Lys-25**) is denoted by an asterisk.

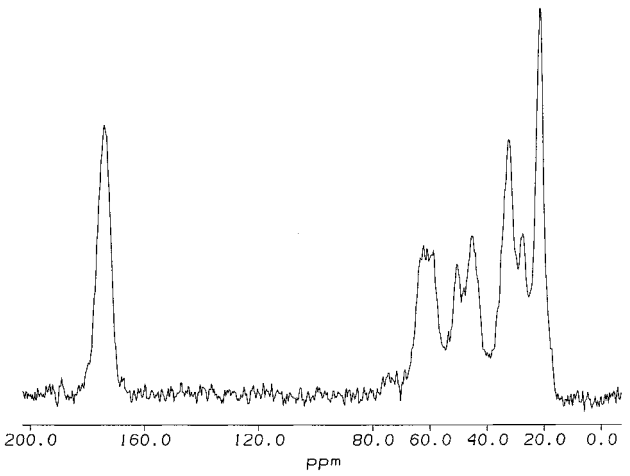

Figure 4. Solid-state CP/MAS ^{13}C NMR spectrum of a lyophilized specimen of poly(**Lys-25**).

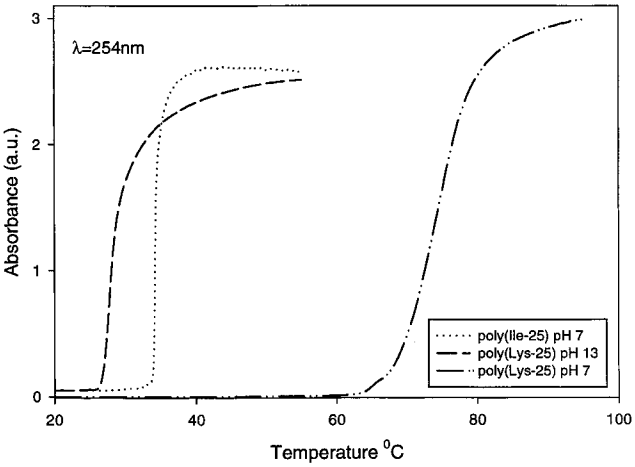

Figure 5. Temperature-dependent turbidimetry profiles for solutions of poly(**Lys-25**) in water (pH 7) and 10 mM NaOH solution (pH 13). The turbidimetric profile of poly(**Ile-25**) in water (pH 7) is included for comparison.

compositional analyses of poly(**Lys-25**) and poly(**Ile-25**) were consistent with polymers of repeat units **1** and **2**, respectively. The repeat unit of poly(**Lys-25**) was confirmed additionally by N-terminal amino acid sequence analysis and MALDI−TOF mass spectrometry of the proteolytic fragment derived from site-specific cleavage of the protein polymer with *Lys-C* endoproteinase.[11] The MALDI−TOF mass spectra of the intact polypeptides poly(**Lys-25**) and poly(**Ile-25**) gave broadened peaks centered at 80 645 and 33 047 Da, respectively. The spectrometric resolution was sufficient to distinguish between the masses of successive repeat units and to determine the degree of oligomerization of the respective polypeptides. The observed masses most closely corresponded to sequences comprising 39 repeats of **1** for poly(**Lys-25**) (expected mass = 81 095 Da) and 16 repeats of **2** (expected mass = 33 099 Da) for poly(**Ile-25**).

The ^1H and ^{13}C NMR spectroscopic data provide strong support for the primary structure of poly(**Lys-25**) and poly(**Ile-25**) (Tables 1 and 2). The individual resonances of the protein polymers are identified from the known chemical shift assignments of poly(Val-Pro-Gly-Val-Gly)[21] and confirmed by $^1H-^1H$ COSY and $^1H-^{13}C$ HMQC NMR spectroscopy of poly(**Lys-25**). The presence of the lysine residue is detected in the ^1H and ^{13}C NMR spectra of the poly(**Lys-25**) at levels commensurate with its percent incorporation into the repeat sequence (Tables 1 and 2).[22,23] In particular, a unique resonance is observed at 176.9 ppm in the ^{13}C NMR spectrum of poly(**Lys-25**) (Figure 3) that does not appear in the corresponding spectra of poly(Val-Pro-Gly-Val-Gly) and poly(**Ile-25**) (Table 2). The position and relative intensity of this resonance are consistent with a lysine carboxamide group within a peptide bond.[22] In addition, the resonances of the amide carbonyl groups for other amino acid residues display microheterogeneity due to the regular substitution of a lysine residue at position 4 in every fifth pentapeptide repeat in poly(**Lys-25**). The most conclusive evidence for the incorporation of a lysine residue into the protein polymer is the presence of a unique resonance at 32.1 ppm in the ^{15}N NMR spectrum of poly(**^{15}N-Lys-25**) at the expected position for the unsubstituted amine groups of the lysine side chains.[23]

The solid-state CP/MAS ^{13}C NMR spectrum of poly(**Lys-25**) suggests that its solution structure is largely maintained in lyophilized specimens based on similar patterns of carbon resonances between the corresponding spectra (Figure 4).

Temperature-Dependent Phase Behavior. The inverse temperature transitions of protein polymers poly(**Lys-25**) and poly(**Ile-25**) in aqueous solution are determined by temperature-dependent turbimetry (Figure 5).[24] In all cases, coacervation of the polypeptides is reversible on lowering the temperature below the observed T_t. For example, a sharply defined, reversible phase transition is observed at approximately 34 °C for aqueous solutions of poly(**Ile-25**) (1 mg/mL) that is essentially independent of pH. In contrast, the phase behavior of poly(**Lys-25**) depends strongly on the pH of the solution due to proton-transfer equilibria involving the lysine residues. The inverse temperature transition observed for poly(**Lys-25**) shifts from 28 °C in 0.1 N NaOH to 75 °C in unbuffered water (Figure 5). The breadth of the latter transition suggests that poly(**Lys-25**) forms a self-buffering solution in water. In contrast, buffered aqueous solutions of poly(**Lys-25**) at neutral pH (50 mM Tris−HCl, pH 7.0) do not coacervate at temperatures below 100 °C, which indicates that protonation of the lysine side chains inhibits coacer-

vation. However, poly(**Lys-25**) displays a sharp, reversible transition at approximately 50 °C in either buffered or unbuffered aqueous solution in the presence of salt (150 mM NaCl). Presumably the salt-induced shift in transition temperature is due to screening of electrostatic repulsion between the charged ammonium groups of the lysine residues. The transition temperatures observed using temperature-dependent turbidimetry agree with those obtained from differential scanning calorimetry (DSC) under identical conditions.[25]

Vrhovski et al.[26] have investigated the effects of solution composition (buffer pH, ionic strength, and polypeptide concentration) on the temperature-dependent coacervation of recombinant human tropoelastin, which contains unmodified lysine residues in the cross-linkable domains. The recombinant tropoelastin did not undergo coacervation in nearly neutral, buffered solution (phosphate buffer, pH 7.4) in the absence of sodium chloride. However, coacervation of recombinant tropoelastin was observed in the physiological temperature range upon addition of sodium chloride (150−200 mM) to the buffered solution. In addition, the transition temperature of the recombinant tropoelastin shifted from 42 to 36 °C as the pH of the phosphate buffer increased from 5.4 to 8.4. These observations correlate well with our results on the coacervation of poly(**Lys-25**) and suggest that coacervation is inhibited by unscreened charge repulsion between protonated lysine residues in both biomaterials.

Synthesis of Elastin-Mimetic Gels. Urry et al., have extensively described the fabrication and physical properties of elastomeric matrices based on elastin-mimetic protein polymers.[16,27] These elastomeric networks have been prepared primarily via γ-radiation-induced, radical cross-linking of the protein polymer in the coacervate state. Although effective for many technological applications, this procedure does not afford gels of regular molecular architecture due to a lack of chemoselectivity in the radical reactions. In addition, the ionizing radiation employed in this process can cause physical damage to the material such as degradation of the polymer backbone. In contrast, the synthesis of elastin-mimetic hydrogels reported herein is based on selective reaction between the ϵ-amino groups of the regularly spaced lysine residues in poly(**Lys-25**) and a bifunctional cross-linker. These reactions can be conducted under mild and controllable conditions with negligible degradation of the protein polymer. Elastin-mimetic networks derived from poly(**Lys-25**) should contain cross-links at well-defined positions *in the limit of complete substitution* of the amino groups, although the formation of intramolecular loops and monosubstituted side chains can occur as side reactions during this process.

The choice of cross-linker has a critical impact on the properties of the polymer gel because it becomes incorporated into the network. Selective cross-linking of lysine residues in biomolecules has been accomplished using a variety of reagents including glutaraldehyde, bis(imidoesters), and *N*-hydroxysuccinimide esters of bifunctional carboxylic acids.[28] Although glutaraldehyde has been used extensively as a cross-linking agent, neither its reaction chemistry nor the chemical identity of the resulting cross-links is well-defined.[29] Bis(imidoesters) are also widely employed for chemical fixation of biological specimens; however, these reagents form positively charged amidinium ions upon reaction with amino groups. The responsive properties of these polyelectrolyte gels can be dominated by electrostatic repulsion between the charged amidinium groups rather than by hydrophobic assembly of the elastin segments. Since most bioelastomeric materials, including elastin, do not have an appreciable charge on the polymer network, this cross-linking chemistry was avoided for the preparation of the hydrogels.[4] *N*-Hydroxysuccinimide esters of bifunctional carboxylic acids were chosen for the preparation of synthetic polypeptide networks on the basis of the following criteria:[30] (1) well-defined reaction chemistry, (2) production of stable, uncharged amide cross-links, and (3) commercial availability of reagents with different spacer compositions and lengths between reactive end groups.

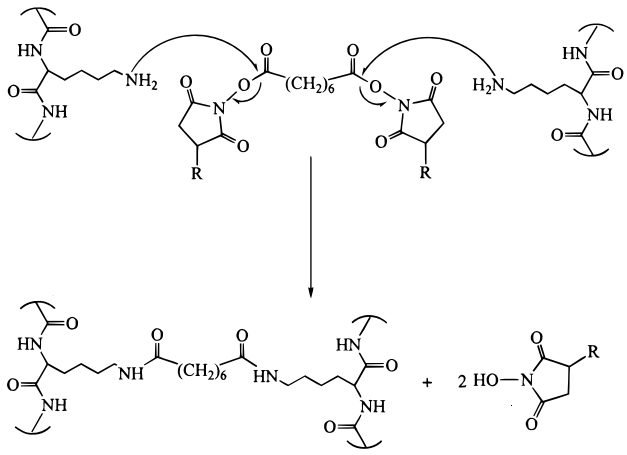

Figure 6. Proposed mechanism of intermolecular cross-link formation in lysine-containing polypeptides via condensation with bis(*N*-hydroxysuccinimidyl) suberates (R = H for dimethyl sulfoxide solution; R = $SO_3^-Na^+$ for aqueous solution).

The cross-linking reaction involves nucleophilic displacement of the *N*-hydroxysuccimide leaving group from the cross-linker by the ϵ-amino group of a lysine residue on the polypeptide to form an amide bond (Figure 6). This reaction is rapid and irreversible at ambient temperature in neutral to slightly basic aqueous solution (pH 7−9) or in polar organic solvents such as dimethyl sulfoxide. When the bifunctional molecule reacts with lysine residues from two different polypeptide chains, an intermolecular cross-link forms between the chains. As the reaction proceeds, the effective degree of intermolecular cross-linking between polypeptide chains approaches the gel point of the mixture. This cross-linking process more closely emulates the biological assembly of elastin in that charged amino groups of lysine residues within the soluble precursor are converted to neutral cross-links during formation of the network.[31] Although the mechanism of cross-link formation differs between the two systems, the cross-linking of poly(**Lys-25**), a relatively simple model of tropoelastin, may provide information regarding the effect of charge neutralization on the assembly of the elastin matrix (vide infra). In addition, the elastin-mimetic networks described herein may possess significantly different structural and mechanical properties than those prepared by Urry et al., since the cross-linking reaction occurs initially in the soluble region of the phase diagram rather than in the coacervate state.

Poly(**Lys-25**) was cross-linked into a gel by treatment of a 5−7.5% (w/v) solution of the polypeptide in either aqueous phosphate buffer or anhydrous dimethyl sulfoxide with a bis(*N*-hydroxysuccinimidyl) derivative of

suberic acid. For reactions under aqueous conditions, the polypeptide was dissolved initially in the buffer at 4 °C, which is well below the transition temperature of poly(**Lys-25**) under these conditions. The cross-linker was added at low temperature and the mixture warmed to 25 °C for the cross-linking reaction. After approximately 10 min in either case, the reaction mixtures formed mechanically stable gels that could be physically manipulated without fragmentation. In contrast, poly(**Ile-25**) did not gel under identical conditions in either aqueous or dimethyl sulfoxide solution. Interestingly, the physical appearance of the poly(**Lys-25**) gels depended on the reaction solvent. The gels formed in dimethyl sulfoxide were optically transparent, while those formed in aqueous buffer at 25 °C were opalescent. The translucence of the latter material suggests that microscopic phase separation (microsyneresis) of the protein polymer occurs during the cross-linking reaction under aqueous conditions (vide infra).[3]

Characterization of Elastin-Mimetic Gels. Comparisons of the spectroscopic data for poly(**Lys-25**) before and after the cross-linking reaction suggests a close structural correlation between the protein precursor and the derived gels. The solid-state CP/MAS ^{13}C NMR spectrum of the lyophilized hydrogel is indistinguishable from that of poly(**Lys-25**). In addition, the FTIR spectra of lyophilized specimens of poly(**Lys-25**) are nearly superimposable before and after the cross-linking reaction. The spectroscopic features in the amide I−III regions of the second-derivative FTIR spectra coincide with the expected vibrational transitions for the β turns of the elastin structure.[32,33] However, a weak absorption is observed at 1615 cm^{-1} in the FTIR spectrum of the lyophilized hydrogel that is absent in the corresponding spectrum of poly(**Lys-25**). This spectroscopic feature is tentatively assigned to the IR absorption of amide groups within cross-links that arise from chemical modification of the lysine side chain during the cross-linking reaction.[34] A nascent amide bond is also detected in the carbonyl region of the ^{13}C NMR spectrum of a water-swollen gel, which is absent in the corresponding spectrum of poly(**Lys-25**) (Figure 3). The chemical shift of this resonance (178.4 ppm) falls within the expected range for a nonpeptidic amide group within an amino acid side chain (cf. Asn γ_{CO}, 177.2 ppm; Gln δ_{CO}, 180.5 ppm).[23] For comparison, the amide carbonyl resonances of the polypeptide backbone of the hydrogel are minimally displaced relative to the poly(**Lys-25**) precursor (Figure 3). Although a reaction clearly occurred between the polymer and cross-linker, the spectroscopic data does not provide a quantitative estimate of the extent of lysine substitution during the cross-linking reaction.

Since residual amino groups can alter the responsive properties of the gel and introduce non-cross-linked defect sites into the network, optimization of the cross-linking reaction was crucial for the formation of gels with uniform microstructure and well-defined responsive behavior. Chemical derivatization and quantitative solid-state NMR spectroscopy were employed to estimate the content of residual amino groups and, therefore, the efficiency of the cross-linking reaction between the bis(*N*-hydroxysuccinimide) esters and poly(**Lys-25**). In the former analysis, the synthetic gels were treated with sulfosuccinimidyl-4-*O*-[4,4′-dimethoxytrityl] butyrate (sulfo-SDTB) under aqueous conditions. This reagent is commonly used for quantitating amine content on solid substrates through generation of dimethoxytrityl cation that can be spectroscopically detected (λ_{max} = 498 nm) with high sensitivity.[15] The residual amino groups are converted into substituted butyramide derivatives, which undergo acid-catalyzed hydrolysis to release the dimethoxytrityl cation (Figure 7). This analysis has the advantage that the analyte is released into solution and can be physically separated and spectroscopically quantified without interference from the gel.

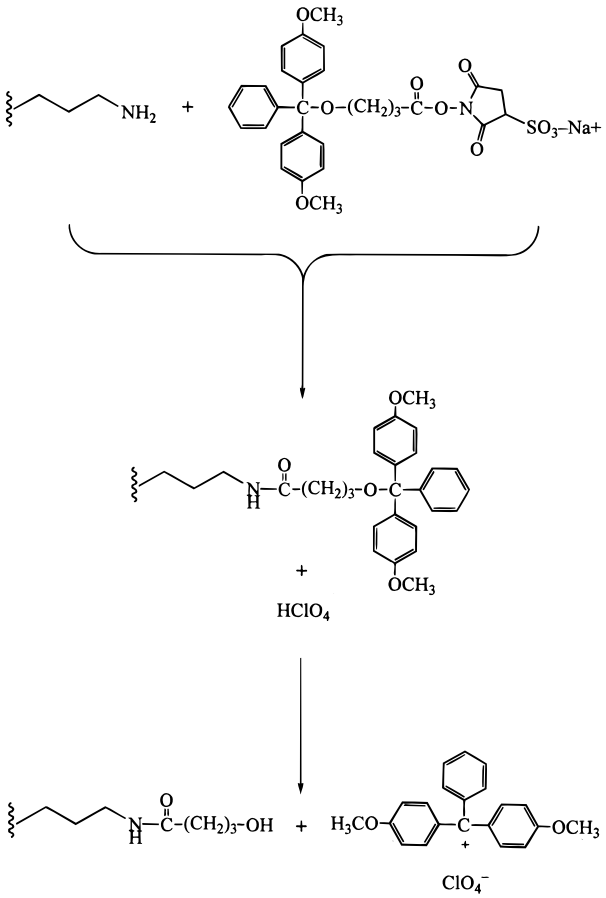

Figure 7. Procedure for the quantitation of residual amino groups in polypeptide hydrogels via reaction with the chromogenic reagent sulfosuccinimidyl-4-*O*-[4,4′-dimethoxytrityl] butyrate (sulfo-SDTB).

The procedure of Cook et al.[15] was employed to construct a calibration curve of standard concentrations of dimethoxytrityl cation (Figure 1). The total amine content of non-cross-linked poly(**Lys-25**) was determined using this analysis and was set as the theoretical 100% value for comparison to the elastin-mimetic gels. This benchmark provided an intrinsic correction for background contributions due to nonspecific association and/or side reactions of the sulfo-SDTB reagent with the protein polymer.[15] On the basis of this assay, the protein gels prepared under aqueous conditions contain 12 ± 3.1% residual amino groups, which indicates an 88% efficiency of substitution of lysine residues during the cross-linking reaction under these reaction conditions. Protein gels prepared from dimethyl sulfoxide solution possess a comparable level (17 ± 2.1%) of residual amino groups within the error limits of this assay. Although this method does not distinguish between monosubstituted and disubstituted derivatives of the cross-linker, the procedure provides an estimate of the upper level of cross-linking efficiency in the network. On the basis

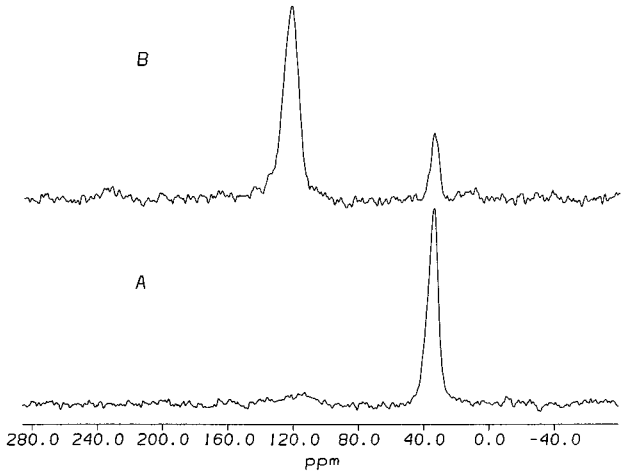

Figure 8. (A) Solid-state VACP/MAS ^{15}N NMR spectrum of poly(**^{15}N-Lys-25**) before the cross-linking reaction. (B) Solid-state VACP/MAS ^{15}N NMR spectrum after the cross-linking reaction.

of repeat sequence **1**, a theoretical cross-link density of 4% (one cross-link per 25 residues) is expected for gels derived from poly(**Lys-25**) in the limit of complete reaction of the amino groups. However, the cross-link density of the synthetic gels cannot exceed maximum derivatization level of the lysine side chains that comprise the cross-links. The derivatization levels correspond to maximal cross-linking efficiencies of 3.5% and 3.3% (within the error limits) for the gels prepared in aqueous buffer and dimethyl sulfoxide, respectively. Although the cross-linking reaction was incomplete, a significant degree of intermolecular cross-linking must have occurred on the basis of this assay and the insolubility and physical integrity of the gels.

The isotopically labeled protein polymer poly(**^{15}N-Lys-25**) was employed in the cross-linking reaction to independently ascertain the extent of lysine derivatization during gel formation by solid-state ^{15}N NMR spectroscopy (Figure 8). Prior to the cross-linking reaction, a single resonance is observed at 34.1 ppm in the solid-state ^{15}N NMR spectrum of poly(**^{15}N-Lys-25**), which is within the expected range for an unsubstituted lysine side chain (cf. 32.1 ppm for the ϵNH_3^+ in the solution phase ^{15}N NMR of poly(**^{15}N-Lys-25**)). After the cross-linking reaction, two resonances of unequal intensity are observed in the ^{15}N NMR spectrum of the lyophilized hydrogel at chemical shifts of 34.1 and 123.9 ppm (Figure 8). The high field resonance has lower intensity and coincides with the single resonance of poly(**^{15}N-Lys-25**). This signal corresponds to residual, unreacted lysine side chains within the hydrogel, the presence of which is expected on the basis of the colorimetric assay (vide supra). The lower field resonance resides within the range for substituted amide groups; although, it is shifted downfield from the typical values for the side chain amide groups of amino acid residues in random coil conformations (cf. Asn γ_N, 112.7 ppm; Gln δ_N, 112.1 ppm).[23] The position of this resonance suggests that it arose from the nascent amide groups within the cross-links of the hydrogel (Figure 6).

The relative proportion of amide vs amino groups within cross-linked poly(**^{15}N-Lys-25**) was determined from the integrated intensity of the individual resonances in the solid-state CP/MAS ^{15}N NMR spectrum of the lyophilized hydrogel. The evolution of nitrogen magnetization for different sets of ^{15}N nuclei was

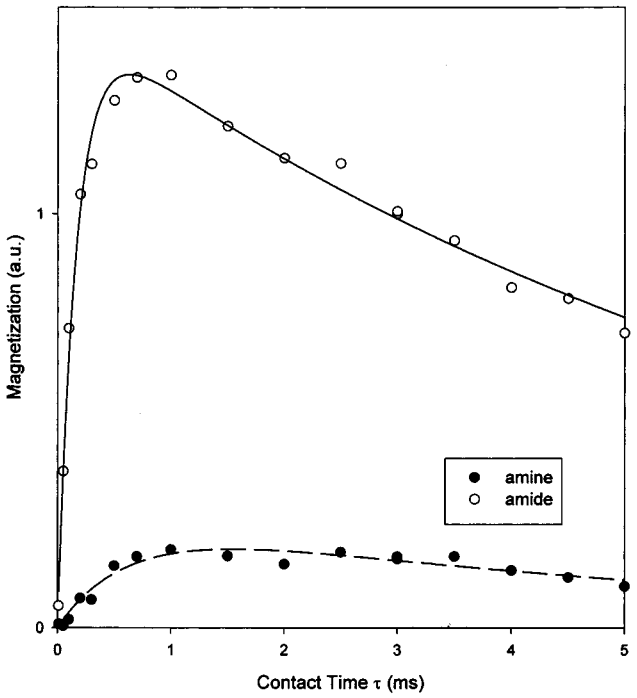

Figure 9. Evolution of the ^{15}N magnetization values for the amide and the amino groups in the CP/MAS ^{15}N NMR spectrum of cross-linked poly(**^{15}N-Lys-25**) as a function of contact time (τ). The solid lines show the best fit to eq 1 for the reacted (amide) and unreacted (amine) lysine side chains of the lyophilized hydrogel.

Table 3. Standard Parameters Derived from Fitting the Evolution of Nitrogen Magnetization as a Function of Contact Time (τ) to Eq 1

sample	resonance (ppm)	M_0 (au)	$T_{1\rho H}$ (ms)	T_{CP} (ms)
poly(**Lys-25**)	34.1	1.054 (0.065)	19.899 (8.392)	0.589 (0.071)
poly(**Lys-25**)	34.1	0.251 (0.031)	5.622 (1.638)	0.624 (0.137)
hydrogel	123.9	1.459 (0.030)	7.264 (0.462)	0.163 (0.01)

measured as a function of contact time (τ).[14] These data were fit to the equation for the standard model to extract the values of M_0 for the reacted (R) and unreacted (U) lysine side chains, 1.459 (0.030) and 0.251 (0.031), respectively (Figure 9). The values of the fitting parameters and the associated standard deviations are summarized in Table 3 for poly(**^{15}N-Lys-25**) before and after the cross-linking reaction. Fractional compositions of 0.853 and 0.147 were calculated from these values for the reacted (amide) and unreacted (amine) sites, respectively. These results agree within experimental error with the relative populations of reacted and unreacted sites determined from the colorimetric analysis with sulfo-SDTB.

Phase Behavior of Elastin-Mimetic Hydrogels. The responsive behavior of the elastin-mimetic hydrogels was investigated most conveniently for thin film specimens (approximate thickness = 0.7 mm) prepared by casting the cross-linking reaction into a mold at 10 °C and curing at 25 °C for 24 h. These hydrogels reversibly expand and contract upon cycling through the phase transition as determined by the change in physical dimensions as a function of temperature (Figure 10). An increase in temperature from 10 to 45 °C results in an isotropic contraction in the dimensions of the hydrogel, which corresponds to a 62.4% reduction in swollen volume. The position of the phase transition for the hydrogel film is determined from the temperature

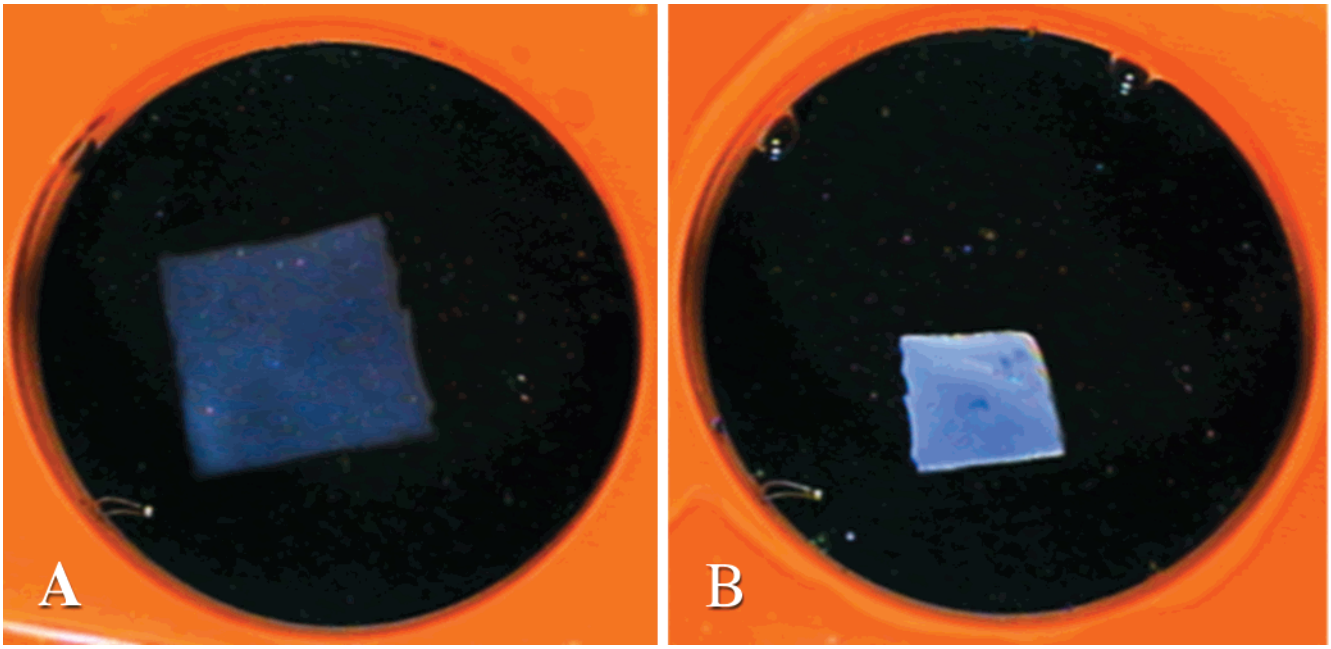

Figure 10. Change in dimensions of a cast film of an elastin-mimetic hydrogel as a function of temperature. The gel specimens were equilibrated in distilled water for 12 h at representative temperatures below (A, 10 °C) and above (B, 45 °C) the phase transition.

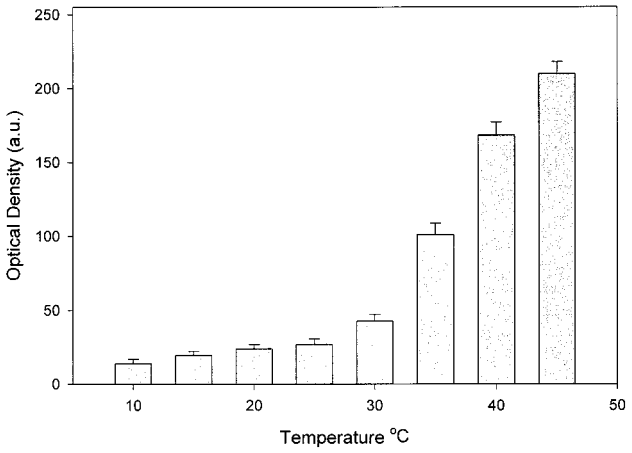

Figure 11. Bar graph depicting the change in the optical density of a hydrogel specimen as a function of temperature. The hydrogel was equilibrated at each temperature for 1 h before recording the image with a digital camera.

dependence of the optical density (Figure 11). Digital image capture and analysis of the hydrogels indicate a relatively broad, but distinct transition with an estimated midpoint temperature of 35 °C. The phase transition occurs at a substantially lower temperature than that of the precursor poly(**Lys-25**) under identical conditions (vide supra), which is consistent with a decrease in polymer−solvent affinity after the cross-linking reaction. Macroscopic hydrogel specimens display similar temperature-dependent, reversible volume transitions. In addition, macroscopic phase separation (macrosyneresis) is clearly evident in bulk specimens at temperatures above the apparent phase transition as indicated by the appearance of a visually distinct aqueous phase.

Urry has described identical phenomena for elastin-mimetic protein polymers cross-linked into elastomeric matrices by γ-irradiation of the coacervate.[16] The position of this phase transition in the cross-linked materials was a function of the polarity, or, more accurately, the hydrophilicity, of the protein polymer. For the homologous series of elastin-mimetic polymers [(Val-Pro-Gly-Xaa-Gly)$_n$], the polarity of the fourth residue (Xaa) of the pentapeptide repeat served as a convenient index of the polymer−solvent interaction.[24] The phase transition shifted toward higher temperatures in a reproducible and quantifiable manner as the hydrophilicity of the amino acid (Xaa) increased due to enhanced affinity between the polypeptide and the aqueous solvent. Because the cross-linking of poly(**Lys-25**) involves the conversion of the charged, hydrophilic amino groups into uncharged, less polar amide groups (Figure 6), a decrease in the value of T_t is expected for the hydrogels vis-à-vis the parent polymer poly(**Lys-25**) as a result of the decrease in hydrophilicity of the amino acid substituent groups.

The magnitude of the expected shift in the value of T_t for the hydrogel can be estimated from the amino acid hydrophobicity correlations determined by Urry et al. from the phase behavior of the protein polymers [(Val-Pro-Gly-Xaa-Gly)$_n$].[24] The glutamine residue is used in these calculations as a stereoelectronic approximation of the nascent amide side chains within the hydrogel that arise during the cross-linking reaction of poly(**Lys-25**). Under this assumption, the conversion of amine side chains to amide side chains should depress the phase transition by approximately 60 °C based on the ΔT_t between [(Val-Pro-Gly-Lys-Gly)$_n$] (estimated T_t = 120 °C) and [(Val-Pro-Gly-Gln-Gly)$_n$] (estimated T_t = 60 °C). However, these transition temperatures represent 100% incorporation of the polar residues (Xaa), and lower levels of incorporation would shift the T_t's to lower temperatures in accordance with Urry's observations. At a level of 20% Gln incorporation in the repeat, the transition temperature of the protein polymer should decrease to 33 °C as determined from Urry's linear relationships of fractional residue content vs T_t in the polypeptide series [(Val-Pro-Gly-{Xaa$_{(x)}$/Val$_{(1-x)}$}-Gly)$_n$]. The fractional amide content in this synthetic sequence approximates that determined for hydrogels derived

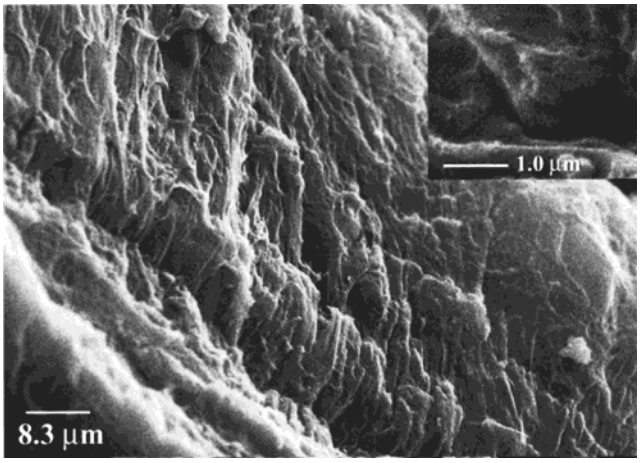

Figure 12. SEM image of a protein gel prepared by reaction of poly(**Lys-25**) with a stoichiometrically equivalent amount of the cross-linker disuccinimidyl suberate in anhydrous dimethyl sulfoxide. The inset displays a higher magnification image of the same region of the gel.

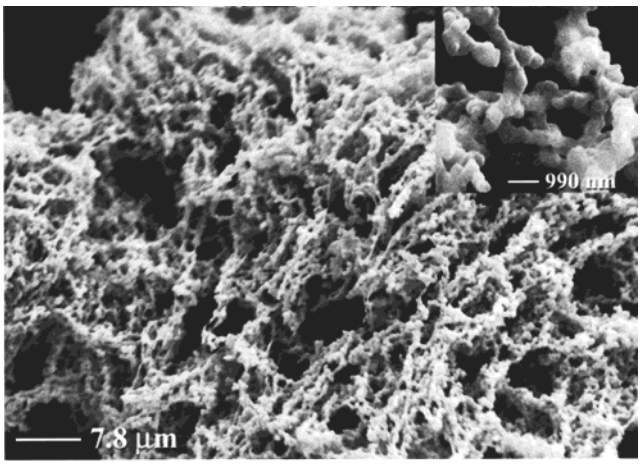

Figure 13. SEM image of a protein gel prepared by reaction of poly(**Lys-25**) with a stoichiometrically equivalent amount of the cross-linker bis(sulfosuccinimidyl) suberate in phosphate buffer. Notice the beaded morphology of the elastin fibrils within the magnified image depicted in the inset.

from cross-linking poly(**Lys-25**). Thus, the phase transition observed for the poly(**Lys-25**) hydrogel temperature (35 °C) closely approaches the calculated value derived from a chemosynthetic polypeptide of similar amino acid composition.

Solvent Effects on Gel Microstructure. The morphology of the elastin mimetic gels was investigated by high-resolution scanning electron microscopy. Gel specimens were dried under supercritical conditions after solvent exchange with carbon dioxide and coated with a thin layer of a Au/Pd alloy prior to image acquisition. Although this treatment may have introduced structural artifacts into the specimens,[35] the dramatic differences in morphology observed between elastin-mimetic protein gels prepared under nonaqueous conditions vs aqueous conditions are presumably intrinsic to the materials since the fixation procedures were nearly identical between the two specimens (Figures 12 and 13). The protein gel prepared in dimethyl sulfoxide has a homogeneous morphology in which individual filaments are densely packed into a monolithic structure (Figure 12). The uniform microstructure of this specimen suggests that poly(**Lys-25**) is chemically cross-linked into a network without concomitant phase separation, i.e., gelation occurs within the homogeneous region of the polymer−solvent phase diagram. In contrast, the morphology of the gel prepared in aqueous solution consists of an inhomogeneous network of interconnected beaded filaments with nodular features on the order of several hundred nanometers in diameter (Figure 13). An irregular pore structure is observed within this specimen at low magnification, which suggests that microscopic phase separation occurs during the cross-linking reaction. At higher magnification, the connections between beaded filaments are more clearly discerned in the specimen, in which individual filaments become entangled within an interconnected network (Figure 13 inset). This microstructure is representative of the global morphology of the gel since imaging at several sites within the specimen reveals nearly identical features.

The differences in morphology observed between the two gel specimens presumably result from differences in interactions between the protein polymer and the swelling solvent during the cross-linking reaction. Both elastin-mimetic protein gels have nearly identical chemical compositions, which are independent of the solvent identity, in the ideal limit of 100% substitution of the lysine amino groups. Although the latter process is incomplete in each case, the estimated contents of residual amines, and, presumably, the upper limits of cross-link formation, are comparable for the two elastin-mimetic gels. The single-phase morphology of the gel prepared in dimethyl sulfoxide suggests a favorable polymer−solvent interaction before and after the cross-linking reaction such that negligible microphase separation occurs during gelation. In support of this assumption, neither poly(**Lys-25**) nor poly(**Ile-25**) display a temperature-dependent phase transition in dimethyl sulfoxide over the temperature range from 20 to 100 °C. Both polypeptides are within the homogeneous region of the phase diagram despite the large difference in side chain polarity between the periodic isoleucine and lysine residues within the two protein polymers. Therefore, conversion of the amino group of lysine to a less polar amide during the cross-linking reaction neither significantly alters the polymer−solvent interaction nor initiates microphase separation in dimethyl sulfoxide.

In contrast, most elastin-mimetic polypeptides exhibit a phase transition in aqueous solution in which the transition temperature T_t depends strongly on the polarity of the amino acid residues (Xaa) of the pentapeptide repeats. For example, the phase transition for poly(**Lys-25**) shifts nearly 50 °C depending on the pH of the solution and, ultimately, the charge state of the lysine side chain. During the cross-linking reaction, the charged ammonium groups of the lysine residues are converted to uncharged amide groups, which results in a significant decrease in the transition temperature (vide supra). However, the cross-linking process probably does not occur uniformly and simultaneously throughout the system since concentration fluctuations within the reaction mixture can cause local variation in the reaction rates between the lysine groups and the cross-linker. As the reaction proceeds, the affinity of local segments of the polymer backbone for the aqueous solvent should decrease due to derivatization of the lysine residues. These polymer segments can aggregate within these localized domains and precipitate from the reaction mixture. The effective attraction between poly-

mer chains induced by the cross-linking process should enhance the microscopic phase separation. This pattern of microsyneresis is spatially preserved in the material after the onset of gelation and is detected in the morphology of the gel by electron microscopy (Figure 13).[3]

Microscopic phase separation has been employed previously for the synthesis of microporous materials having open cell microstructures.[36] Phase separation was usually induced in the nascent gel by raising the reaction temperature above the LCST during the cross-linking reaction.[37] The microsyneresis of the network reflected the evolution of spinodal decomposition in the cross-linking reaction immediately prior to gelation. The pore structure that evolved within these materials depended on several factors including the initial polymer concentration and the temperature program employed during the cross-linking reaction.[38] In contrast, the microscopic phase separation observed in the elastin-mimetic hydrogels results from a change in the polymer−solvent interaction during the cross-linking reaction rather than a temperature-induced phase separation. Modification of the lysine side chains decreases the hydrophilicity of the polymer segments, which causes localized precipitation of the gel. In other words, the position of the spinodal envelope for the polymer−solvent mixture is effectively shifted toward the reaction temperature as the cross-linking reaction proceeds to completion. Although the reaction temperature is still above the observed transition temperature of the hydrogel, the proximity of the phase transition may induce microsyneresis within the evolving network structure. In support of this hypothesis, Sciortino et al. demonstrated that damped concentration fluctuations initiated fiber formation in aqueous solutions of (Val-Pro-Gly-Val-Gly)$_n$ (n_{avg} > 120) as the spinodal line was approached from the region of stability in the phase diagram.[17] This process probably occurred via a nucleation-growth mechanism, in which local concentration fluctuations induced the formation of propagating elastin nuclei. However, we cannot distinguish between alternative mechanisms for microphase separation in the elastin-mimetic hydrogels solely on the basis of the SEM data.

Because recombinant human tropoelastin has similar phase behavior to poly(**Lys-25**) in vitro, the cross-linking studies of poly(**Lys-25**) suggest that tropoelastin should exhibit microscopic phase separation during the assembly of elastic fiber under physiological conditions. However, the microstructure of native elastic fiber in vivo comprises a densely packed matrix of beaded filaments of cross-linked tropoelastin with no evidence for microsyneresis.[39] The in vivo deposition of elastic fiber is tightly regulated to afford the desired elastin ultrastructure and prevent the formation of less ordered, alternative structures.[31] The deposition process involves the intermediacy of other biomolecules to control the nucleation and growth of the elastin matrix. Microfibrillar proteins act as a scaffold for the deposition of tropoelastin, which is regulated through specific protein−protein interactions.[40] In addition, an elastin binding protein prevents the premature aggregation of tropoelastin, and facilitates the controlled deposition of elastic fiber.[41] Process control obviously plays an important role in the deposition of elastic fiber, and emulation of the natural fiber assembly process may afford better fabrication methods for synthetic elastin analogues for biomedical applications.

Conclusions

The goal of this research is the preparation of polymer gels of well-defined microstructure via chemical cross-linking of an elastin-mimetic protein polymer, poly(**Lys-25**), that contain periodic lysine residues at uniform intervals. The greater uniformity of network architecture, i.e., macromolecular size, cross-link position, and cross-link density, that is available in protein polymers may lead to greater control over the macroscopic properties of responsive gels derived from biosynthetic polypeptides. Indeed, the uniform structure of the precursor protein poly(**Lys-25**) permits a more detailed evaluation of the primary structure of the gel than is commonly possible for most synthetic polymer gels. Spectroscopic investigations of the polymer gels indicate that the cross-linking reaction proceeds exclusively through the lysine side chains of the protein polymer, and allow for an estimation of the degree of substitution of the amino groups. Although the cross-linking reaction is incomplete, formation of mechanically stable, environmentally responsive gels is observed under the reaction conditions. The shift in the phase transition for the hydrogel is understood in terms of the local conversion of lysine side chains from amines to amides during the cross-linking reaction. The absolute cross-link density is not determined from these studies; although, an upper limit is estimated based on the percent conversion of lysine side chains. However, the density of elastically effective cross-links can be determined from stress−strain measurements on gel specimens and related to the theoretical maximal cross-link density derived from the calculation of percent conversion of the amine groups of lysine residues.[42,43] Uniaxial compression studies on gel specimens of defined dimensions are currently in progress to evaluate the effective cross-link density of these elastin-mimetic materials.[44] The precise molecular architecture of poly(**Lys-25**) aids in the interpretation of these analyses, and in this sense, provides a uniform context for evaluation of the structure−property relationships within polymer hydrogels.

This study also demonstrates that the morphology of a gel is not solely a function of the molecular structure of the polymer precursor as changes in the polymer−solvent interaction during the cross-linking reaction dramatically modify the three-dimensional architecture of gels prepared in dimethyl sulfoxide vs aqueous solution despite the structural uniformity of poly(**Lys-25**). However, the decrease in transition temperature and associated microphase separation of the elastin-mimetic hydrogel can be rationalized in terms of the substituent effects on phase behavior that were determined by Urry et al. for elastin mimetic polypeptides.[24] Therefore, the precisely defined structure of the protein polymer permits a more rational evaluation of the effects of reaction conditions on the microstructure and materials properties of the derived gels. Because the rate of the volume transition depends strongly on the degree of microphase separation within the hydrogel, this approach may have technological utility for fabrication of gels with well-defined responsive behavior through manipulation of reaction parameters that modulate the polymer−solvent interaction including the cross-linker chemistry, the solvent composition, and the reaction temperature.[38]

Acknowledgment. The authors acknowledge the financial support of the Molecular Design Institute of the Georgia Institute of Technology, the Herman Frasch Foundation of the American Chemical Society, and the NASA Office of Life and Microgravity Sciences and Applications (NAG8-1579). The authors thank Dr. Robert Apkarian and Mr. Kevin Caran of the Integrated Microscopy and Microanalytical Facility (IM&MF) of Emory University for SEM images depicted in Figures 12 and 13 and for valuable advice on specimen preparation and SEM image acquisition and processing. The authors thank Dr. Johannes Leisen for assistance in acquisition of the solid-state NMR spectroscopic data, and Mr. Yuri Zimenkov for technical assistance. The authors also thank Professor Stevin Gehrke for helpful discussions and ongoing comments on this research.

References and Notes

(1) Dumitrui, S.; Dumitrui-Medvichi, C. In *Polymeric Biomaterials*; Dumitrui, S., Ed.; Marcel Dekker: New York, 1994; pp 3−97.
(2) Gehrke, S. H.; Fisher, J. P.; Palasis, M.; Lund, M. E. *Ann. N.Y. Acad. Sci.* **1997**, *831*, 179−207.
(3) Matsuo, E. S.; Orkisz, M.; Sun, S.-T.; Li, Y.; Tanaka, T. *Macromolecules* **1994**, *27*, 6791−6796.
(4) Gosline, J. M. *Symp. Soc. Exp. Biol.* **1980**, *34*, 332−357.
(5) Vincent, J. *Structural Biomaterials*; Princeton University Press: Lawrenceville, NJ, 1990; pp 37−72.
(6) (a) Heslot, H. *Biochimie* **1998**, *80*, 19−31. (b) Ferrari, F. A.; Cappello, J. In *Protein-Based Materials*; McGrath, K., Kaplan, D., Eds.; Birkhauser: Boston, MA, 1997; pp 37−60. (c) Cappello, J.; Ferrari, F. In *Plastics from Microbes: Microbial Synthesis of Polymers and Polymer Precursors*; Mobley, D. P., Ed.; Hanser/Gardner Publications: Munich, Germany, 1994; pp 35-92. (d) Tirrell, J. G.; Fournier, M. J.; Mason, T. L.; Tirrell, D. A. *Chem. Eng. News* **1994**, *72*, 40−51. (e) O'Brien, J. P. *Trends Polym. Sci.* **1993**, *1*, 228−232.
(7) Krejchi, M. T.; Atkins, E. D. T.; Waddon, A. J.; Fournier, M. J.; Mason, T. L.; Tirrell, D. A. *Science* **1994**, *265*, 1427−1432.
(8) Yu, S. M.; Conticello, V. P.; Zhang, G.; Kayser, C.; Fournier, M. J.; Mason, T. L.; Tirrell, D. A. *Nature* **1997**, *389*, 167−170.
(9) Petka, W. A.; Harden, J. L.; McGrath, K. P.; Wirtz, D.; Tirrell, D. A. *Science* **1998**, *281*, 389−392.
(10) Tirrell, J. G.; Tirrell, D. T.; Fournier, M. J.; Mason, T. L. In *Protein-Based Materials*; McGrath, K., Kaplan, D., Eds.; Birkhauser: Boston, MA, 1997; pp 61−99.
(11) McMillan, R. A.; Lee, T. A. T.; Conticello, V. P. *Macromolecules* **1999**, *32*, 3643−3648.
(12) Sambook, J.; Fritsch, E. F.; Maniatis, T. *Molecular Cloning: A Laboratory Manual*, 2nd ed.; Cold Spring Harbor Laboratory Press: Cold Spring Harbor, NY, 1989.
(13) Wishart, D. S.; Bigam, C. G.; Yao, J.; Abilgaard, F.; Dyson, H. J.; Oldfield, E.; Markley, J. L.; Sykes, B. D. *J. Biomol. NMR* **1995**, *6*, 135−140.
(14) Rethwisch, D. G.; Jacintha, M. A.; Dybowski, C. R. *Anal. Chim. Acta* **1993**, *283*, 1033−1043.
(15) Cook, A. D.; Pajvani, P. B.; Hrkach, J. S.; Cannizzaro, S. M.; Langer, R. *Biomaterials* **1997**, *18*, 1417−1424.
(16) (a) Urry, D. W. *J. Protein Chem.* **1988**, *7*, 1−34. (b) Urry, D. W. *Angew. Chem., Int. Ed. Engl.* **1993**, *32*, 819−841. (c) Urry, D. W.; Luan, C.-H.; Harris, C. M.; Parker, T. M. In *Protein-Based Materials*; McGrath, K., Kaplan, D., Eds.; Birkhauser: Boston, MA, 1997; pp 133−177.
(17) (a) Sciortino, F.; Prasad, K. U.; Urry, D. W.; Palma, M. U. *Biopolymers* **1993**, *33*, 743−752. (b) Sciortino, F.; Urry, D. W.; Palma, M. U.; Prasad, K. U. *Biopolymers* **1990**, *29*, 1401−1407.
(18) Schild, H. G. *Prog. Polym. Sci.* **1992**, *17*, 163−249.
(19) Flory, P. J. *Principles of Polymer Chemistry*; Cornell University Press: Ithaca, NY, 1953.
(20) McPherson, D. T.; Xu, J.; Urry, D. W. *Protein Expression Purif.* **1996**, *7*, 51−57.
(21) (a) Urry, D. W.; Krishna, N. R.; Huang, D. H.; Trapane, T. L.; Prasad, K. U. *Biopolymers* **1989**, *28*, 819−833. (b) Chang, D. K.; Venkatachalam, C. M.; Prasad, K. U.; Urry, D. W. *J. Biomol. Struct. Dyn.* **1989**, *6*, 851−858. (c) Urry, D. W.; Long, M. M. *CRC Crit. Rev. Biochem.* **1976**, *4*, 1−45.
(22) Wishart, D. S.; Sykes, B. D. *J. Biomol. NMR* **1994**, *4*, 171−180.
(23) Wishart, D. S.; Bigam, C. G.; Holm, A.; Hodges, R. S.; Sykes, B. D. *J. Biomol. NMR* **1995**, *5*, 67−81.
(24) (a) Urry, D. W.; Gowda, D. C.; Parker, T. M.; Luan, C.-H. Reid, M. C.; Harris, C. M.; Pattanaik, A.; Harris, R. D. *Biopolymers* **1992**, *32*, 1243−1250. (b) Urry, D. W.; Luan, C.-H.; Parker, T. M.; Gowda, D. C.; Prasad, K. U.; Reid, M. C.; Safavy, A. *J. Am. Chem. Soc.* **1991**, *113*, 4346−4348.
(25) McMillan, R. A.; Cooper, A.; Conticello, V. P. Unpublished results.
(26) Vrhovski, B.; Jensen, S.; Weiss, A. S. *Eur. J. Biochem.* **1997**, *250*, 92−98.
(27) Elastin-mimetic protein polymers have been chemically crosslinked via a crossed condensation of lysine and glutamic acid residues in the chemosynthetic polypeptides (Val-Pro-Gly-{Xaa/Val}-Gly)$_n$ (Xaa = Glu or Lys) to form N$^{\epsilon}$-(γ-glutamyl)-lysine isodipeptide linkages (Urry, D. W.; Okamota, K.; Harris, R. D.; Hendrix, C. F.; Long, M. M. *Biochemistry* **1976**, *15*, 4083−4089.). The extent of cross-link formation was not quantified for the network in this study.
(28) Wong, S. S. *Chemistry of Protein Conjugation and Cross-linking*; CRC Press: Boca Raton, FL, 1991.
(29) The cross-linking reaction of a terminally functionalized elastin-mimetic protein polymer with glutaraldehyde was reported while this manuscript was in review (Welsh, E. R.; Tirrell, D. A. *Biomacromolecules* **2000**, *1*, 23−30.).
(30) Staros, J. V. *Biochemistry* **1982**, *21*, 3950−3955.
(31) Mecham, R. P.; Davis, E. C. In *Extracellular Matrix Assembly and Structure*; Yurchenco, Y., Birk, D. E., Mecham, R. P., Eds.; Academic Press: San Diego, CA, 1994; pp 281−314.
(32) Thomas, G. J., Jr.; Prescott, B.; Urry, D. W. *Biopolymers* **1987**, *26*, 921−934.
(33) Hollosi, M.; Majer, Z. S.; Ronai, A. Z.; Magyar, A.; Medzihradsky, K.; Holly, S.; Perczel, A.; Fasman, G. D. *Biopolymers* **1994**, *34*, 177−185.
(34) Krimm, S.; Bandeker, J. *Adv. Prot. Chem.* **1986**, *38*, 181−364.
(35) Hydrogels derived from cross-linking poly(**Lys-25**) with bis-(sulfosuccinimidyl) suberate have been imaged under hydrated conditions by cryoscopic high-resolution scanning electron microscopy (cryo-HRSEM).[45] The microstructures observed in the images are commensurate with the morphology of native elastic fiber. (McMillan, R. A.; Caran, K. L.; Apkarian, R. P.; Conticello, V. P. *Macromolecules* **1999**, *32*, 9067−9070.)
(36) (a) Bansil, R.; Liao, G. *Trends Polym. Sci.* **1997**, *5*, 146−154. (b) Nunes, S. P.; Inoue, T. *J. Membr. Sci.* **1996**, *111*, 93−103.
(37) Gehrke, S. H. *Adv. Polym. Sci.* **1993**, *110*, 81−144.
(38) Kabra, B. G.; Gehrke, S. H.; Spontak, R. J. *Macromolecules* **1998**, *31*, 2166−2173.
(39) (a) Pasquali-Ronchetti, I.; Alessandrini, A.; Baccarani-Contri, M.; Fornieri, C.; Mori, G.; Quaglino, D., Jr.; Valdrè, U. *Matrix Biol.* **1998**, *17*, 75−83. (b) Pasquali-Ronchetti, I.; Fornieri, C.; Baccarani-Contri, M.; Quaglino, D. *Ciba Found. Symp.* **1995**, *192*, 31−42. (c) Mecham, R. P.: Heuser, J. E. In *Cell Biology of the Extracellular Matrix*; Hay, E. D., Ed.; Plenum Press: New York, 1991; pp 79−109.
(40) (a) Robb, B. W.; Wachi, H.; Schaub, T.; Mecham, R. P.; Davis, E. C. *Mol. Biol. Cell.* **1999**, *10*, 3595−3605. (b) Brown-Augsburger, P.; Broekelmann, T.; Rosenbloom, J.; Mecham, R. P. *Biochem. J.* **1996**, *318*, 149−155.
(41) (a) Hinek, A.; Keeley, F.; Callahan, J. W. *Exp. Cell Res.* **1995**, *220*, 1−13. (b) Hinek, A.; Rabinovitch, M. *J. Cell Biol.* **1994**, *126*, 563−574.
(42) Tobolsky, A. V.; Carlson, D. W.; Indictor, N. *J. Polym. Sci.* **1961**, *54*, 175−192.
(43) Peppas, N. A.; Barr-Howell, B. D. In *Hydrogels in Medicine and Pharmacy, Vol. I: Fundamentals*; Peppas, N. A., Ed.; CRC Press: Boca Raton, FL, 1986; pp 27−56.
(44) Olivviera, E.; Gehrke, S. H. Private communication.
(45) Apkarian, R. P.; Caran, K. L.; Robinson, K. A. *Microsc. Microanal.* **1999**, *5*, 197−207.

MA9921091